Journal of Polymers and the Environment (2022) 30:2066–2076
https://doi.org/10.1007/s10924-021-02329-6

ORIGINAL PAPER

Preparation of Bacterial Cellulose Fungicide Nanocomposite Incorporated with MgO Nanoparticles

Mohsen Safaei[1,2] · **Mojtaba Taran**[2]

Accepted: 2 November 2021 / Published online: 15 November 2021

Abstract

In recent years, increased consumption of broad-spectrum antimicrobial compounds has enhanced the resistance of various pathogens, including fungi, to existing drugs. Therefore, finding effective and novel compounds that have high antifungal activity are essential. The present research was aimed to exploring the optimum conditions for synthesis of novel nanocomposites containing MgO nanoparticles (NPs) in the cellulose biopolymer matrix with highest antifungal activity. For this purpose, nine experiments were designed using Taguchi method and employing different ratios of cellulose biopolymer and MgO NPs at different stirring times. The synthesized nanocomposite and its components were evaluated by ultraviolet–visible spectroscopy, Fourier transform infrared spectroscopy, X-ray powder diffraction, high-resolution field emission scanning electron microscopy, energy dispersive X-ray spectroscopy, and transmission electron microscopy. The results of the structural analysis, including phase identification, crystal structure, chemical properties, appearance, and particle size, confirmed the formation of cellulose-MgO nanocomposite and improvement of its characterization. The bionanocomposite produced with 4 mg/ml MgO, 1 mg/ml cellulose and 90 min stirring time showed the highest antifungal activity and prevented the growth of fungus *Aspergillus niger* by 85.03%. The results of colony forming unit and disc diffusion showed improvement of antifungal activity of cellulose-MgO nanocomposite compared to its components. Based on the results of the present study, the formation of cellulose-MgO nanocomposite by preventing agglomeration of MgO NPs and enhancing their contact surfaces, improves the antifungal activity of these NPs.

Keywords Nanocomposite · Cellulose biopolymer · MgO nanoparticles · Antifungal activity · Taguchi methods

Introduction

Nowadays, finding favorable treatment for cancer, autoimmune diseases and antimicrobial resistance is among serious challenges of health field [1–4]. Microbial resistance has been increasing rapidly in recent decades. The rate of mortality caused by microbial resistance is expected to reach about 10 million people per year by 2050. Fungal infections are resistant to many drugs used to treat them. Each year more than one and a half million people die because of fungal infections, and this mortality rate is increasing with the sustained drug resistance of fungi [5]. The *Aspergillus niger* is a pathogenic fungus with high distribution in various environmental conditions that has showed a resistant to existing antifungal compounds [6]. Therefore, finding effective and novel compounds that have high antifungal activity against this pathogen urgently required. In recent years, nano products have been widely used for preventing and coping with infectious diseases [7, 8]. On the other hand, natural polymers have been developed and applied in biomedicine due to their biocompatibility [9]. Cellulose is one of the most widely used biopolymers; it is a biocompatible compound applied as an inexhaustible raw material. Bacterial cellulose is a biopolymer with high purity that is used as a promising alternative to plant cellulose (wood fibers and lignocellulosic materials) for specific purposes such as pharmaceutical, food and medical applications. The most important microorganism that produces bacterial cellulose, is *Gluconacetobacter xylinum* that is used to produce cellulose for basic and applied studies [10]. Metal NPs with a size less than 100 nm have better antimicrobial properties than

✉ Mojtaba Taran
mojtabataran@yahoo.com

[1] Advanced Dental Sciences Research Center, School of Dentistry, Kermanshah University of Medical Sciences, Kermanshah, Iran

[2] Department of Biology, Faculty of Science, Razi University, Kermanshah, Iran

micro-size and larger size particles due to the increase in their surface area [11, 12]. Nanoparticles are widely used as fungicides and they can be used in various sectors such as medicine, dentistry, pharmacy, food, textile, environment and agriculture. Various nanoparticles such as silver, titanium dioxide and zinc oxide nanoparticles have shown suitable antimicrobial activities. However, these nanoparticles raise significant concerns about their toxicity due to the dangers connected with heavy metal elements and their cumulation in the body.

In contrast, MgO NPs are a notable alternative to heavy metal based nanoparticles as antimicrobial agent. Because MgO can be broken down and metabolized in the body. As long as renal function is normal, it is effectively removed from the body, thus eliminating the worry of excessive metal cumulation in the body [13].

Along with all the aforementioned benefits, metal NPs have a strong tendency to agglomerate, which is a major limitation for their industrial use. Recently, to overcome this issue, the use of nanoparticles in a stabilizer polymers matrix has been favored due to their distinct properties such as low electrical resistance, good mechanical stability, chemical stability and thermal stability [14, 15]. Polymer-metal nanocomposites have obvious advantages, so that the use of stabilizer polymers prevents agglomeration of metal NPs through stabilizing them and increasing their contact surface [16, 17]. As the use of nanoparticles in the form of nanocomposites improves their contact surface and increases their antifungal activity, these compounds can be used as an alternative to commonly used drugs. Achieving the optimal efficacy of nanocomposites as modern drugs requires systematic and targeted laboratory experiments. To reduce the cost and time of these experiments, the Taguchi method can be very useful.

In this research, the optimal conditions for the targeted synthesis of novel nanocomposite containing MgO NPs in the cellulose bacterial biopolymer matrix with the highest antifungal activity by Taguchi method were evaluated. The antifungal activity of cellulose-MgO nanocomposite against *Aspergillus niger* was investigated using colony forming unit and disc diffusion methods. Characterizations of synthesized biopolymer, nanoparticles and nanocomposite were evaluated by ultraviolet–visible spectroscopy, Fourier transform infrared spectroscopy, X-ray diffraction, scanning electron microscopy, energy dispersive X-ray spectroscopy and transmission electron microscopy.

Materials and Methods

Materials

Magnesium nitrate [$Mg(No_3)_2$] (Sigma-Aldrich 13446-18-9), sodium hydroxide (NaOH) (Sigma-Aldrich 1310-73-2), potassium bromide (KBr) (Sigma-Aldrich 7758-02-3), potato dextrose agar (PDA) (Sigma-Aldrich 70,139), sulphuric acid (H_2SO_4) (Sigma-Aldrich 7664-93-9), ethanol (CH_3CH_2OH) (Sigma-Aldrich 64-17-5), glucose ($C_6H_{12}O_6$) (Sigma-Aldrich 50-99-7), peptone (Sigma-Aldrich 73049-73-7), yeast extract (Sigma-Aldrich 8013-01-2), disodium phosphate (Na_2HPO_4) (Sigma-Aldrich 7558-79-4), and citric acid (C_6H8O_7) (Sigma-Aldrich 77-92-9) were used in this work.

Synthesis of MgO NPs

Co-precipitation method was used to synthesize MgO NPs. For this purpose, 100 mL of 0.1 M $Mg(NO_3)_2$ and 1 M NaOH solution were separately stirred on the magnetic stirrer for 1 h to obtain a uniform solution. Then, two solutions were combined and the resulting solution was continuously stirred at 40 °C for 60 min to obtain a milky solution. After washing and filtration for three times to remove impurities, the resulted precipitate was put in the oven at 60 °C and to obtain $Mg(OH)_2$ powder. Then, to synthesize the MgO NPs, the resulting powder was calcined in the oven at 450 °C for 2 h [18, 19].

Synthesis of Cellulose Biopolymer

The *Acetobacter xylinum* bacterium (PTCC 1734) was provided from the Iranian Scientific and Industrial Research Organization. The microbial cellulose was prepared via modified method described by Nguyen et al. [20]. Briefly, Hestrin-Schramm culture medium was used for culturing bacteria under the static conditions for a week. Then, the grown cellulose layer was collected from the surface of culture medium and placed in sodium hydroxide (0.5 M) solution at 90 °C for 60 min. The resulting cellulose was washed with deionized water and dried at 40 °C until the powder was obtained.

Synthesis of Nanocomposites

To determine the optimal conditions for the synthesis of nanocomposites with the highest antifungal activity, nine experiments were designed based on Taguchi method using the Qulitek-4 software. These experiments included different proportions of the biopolymer and nanoparticles at different stirring times (Table 1). For this purpose, 9 nanocomposites were synthesized to determine their antifungal activity using in situ method and different levels of MgO NPs (2, 4, and 8 mg/ml) and different amounts of cellulose biopolymer (0.5, 1, and 2 mg/ml) at different stirring times of 30, 60, and 90 min. Solutions containing different concentrations of MgO NPs and cellulose polymer were prepared in separate containers according to Table 1. Each solution was then

Table 1 Taguchi design of experiments and fungal growth inhibition rate of cellulose-MgO synthesized nanocomposites

Experiment	MgO (mg/ml)			Cellulose (mg/ml)			Stirring time (min)			Fungal growth inhibition (%)
	2	4	8	0.5	1	2	30	60	90	
1		2			0.5			30		41.38
2		2			1			60		63.69
3		2			2			90		45.83
4		4			0.5			60		73.14
5		4			1			90		85.03
6		4			2			30		68.32
7		8			0.5			90		47.71
8		8			1			30		72.47
9		8			2			60		80.93

sonicated for 10 min until it became uniform. The solutions were combined and stirred for 30, 60, and 90 min at 40 °C to form nanocomposites. Finally, 9 solutions of cellulose-MgO nanocomposites were placed in the oven at 40 °C to prepare their powder [17].

Antifungal Activity

Antifungal activity of synthesized cellulose-MgO nanocomposites against *Aspergillus niger* (ATCC 16404) was studied using CFU and disk diffusion methods. For this purpose, 1 mg/ml of 9 synthesized nanocomposites was added to the solutions containing potato dextrose agar (PDA) and the solutions were transferred to petri dishes. Then, a solution containing about 10^6 CFU/ml was prepared using a fresh colony of *Aspergillus niger* and 100 µL of fungal suspension was cultured in each petri dish. An amount of 100 µL fungal suspension of *Aspergillus niger* was then cultured on a culture medium of potato dextrose agar (without nanocomposite) as the control group. After 96 h incubation at 28 °C, the number of colonies was counted for experimental and control groups. Then, the amount of inhibitory growth of the fungus of each nanocomposite was determined using the following equation:

$$\text{Fungal growth inhibition}\,(\%) = \frac{C_g - E_g}{C_g} \times 100$$

where C_g is the mean growth of colonies in the control group and E_g is the mean growth of colonies in the experimental groups. After determining the optimum conditions for the synthesis of cellulose-MgO nanocomposites with the highest antifungal activity, the antifungal activity of cellulose-MgO nanocomposite, MgO NPs and cellulose biopolymer were compared using two methods of CFU and disk diffusion. In order to compare the antifungal activity of the synthesized compounds, the CFU method was used as same as before. In the disk diffusion method, after preparing the PDA medium, 100 µL of fungal suspension was cultured in each petri dish. Then, disks containing nanoparticles, biopolymer and cellulose-MgO nanocomposite were placed on the culture media. After 48 h of incubation at 28 °C, the amounts of growth inhibition zone were measured by a Vernier caliper. Three tests with three replications were performed for all experiments and their average was reported.

Characterization

The UV spectra of the synthesized compounds (MgO NPs, cellulose biopolymer and cellulose-MgO nanocomposite) were investigated using the Agilent spectrophotometer model 8453. The FTIR spectra of MgO NPs, cellulose biopolymer and cellulose-MgO nanocomposite were recorded in the range of 400–4000 cm^{-1} at room temperature using Fourier transform infrared spectrophotometer model alpha (Bruker, Germany) by providing the KBr tablet. For the evaluation of the crystalline structure of synthesized compounds, the XRD spectra were prepared using a Philips X'Pert device at the incidence angle of 2θ in the range between 10 and 80 degrees. The wavelength of the X-ray copper cathode lamp was 1.54056 Å (40 kV, 30 mA). The size of MgO particles was calculated using the Debye-Scherrer equation. Microstructures of samples were studied using a scanning electron microscope (SEM), model TESCAN (Czech Republic) and transmission electron microscope (TEM) Philips, CM120. The chemical composition analysis of the samples was performed using the energy dispersive X-ray (EDX) detector on the field emission scanning electron microscope (FESEM).

Results and Discussion

UV–Vis Spectroscopy

Characterization of MgO NPs, cellulose biopolymers, and cellulose-MgO nanocomposites was carried by UV–Vis

spectroscopy in the range of 200 to 800 nm (Fig. 1). In the UV spectra of MgO NPs, an absorption peak was observed in the lambda value of 295 nm, which is consistent with previous studies and confirms the synthesis of MgO NPs [21]. There was no absorption band in the cellulose biopolymer spectrum that was consistent with the results obtained by Jiazhi et al. [22]. In comparison to pure components, the absorption spectrum of nanocomposite showed increased intensity and maximum absorption wavelength shifted to 340 nm, indicating the synthesis of nanocomposites. The increase in the amount of wavelength absorbed in the nanocomposite relative to the nanoparticles showed the coating and increase in the diameter of the primary nanoparticles and the formation of the nanocomposite.

FTIR Analysis

Figure 2 shows the FTIR spectra of MgO NPs, cellulose biopolymer and cellulose-MgO nanocomposite in the range of wave number of 400–4000 cm^{-1}. In the spectrum of MgO NPs, the broadband in the range of 3420 cm^{-1} represents the absorption of O–H group through the air [23]. The bands in the range of 1484–1099 cm^{-1} are related to the vibrations of C–O, which is formed from the environment CO_2 absorption. The peaks observed in the range of 867–687 cm^{-1} confirm the binding of magnesium and oxygen [24, 25]. The 3350 cm^{-1} band in the spectrum of cellulose is due to absorption of O–H groups, and the bands at 2900 cm^{-1} and 1370 cm^{-1} refer to the stretching and deformation of C–H group in the structure of glucose. The peak at 1646 cm^{-1} is related to water absorption and the tensile mode of –OH group. The FTIR spectrum at 1431 cm^{-1} is related to the CH_2 symmetric bending vibration. This band is known as crystallization band, and its reduction is equal to the reduction in the degree of crystallinity of the sample. The band observed at about 1162 cm^{-1} is attributed to C–O–C stretching mode of pyranose ring in cellulose. The absorption band at 1059 cm^{-1} is resulted due to C–O– groups of secondary alcohols and existing ether fractions in the cellulose structure, and the signal at 898 cm^{-1} indicates the β-glycosidic links between glucose units forming the cellulose. The peaks at 667 cm^{-1}, 615 cm^{-1}, and 561 cm^{-1} were related to out of plane deformation of hydrogen bonding [26]. The FTIR spectrum of cellulose-MgO nanocomposite showed a combination of properties of cellulose biopolymer and MgO NPs bands. The absorption band at 3418 cm^{-1} represents the formation of hydrogen bond between the hydroxyl group of cellulose biopolymer and MgO NPs. In addition, the changes in wave numbers and size of other peaks indicate a strong link between cellulose biopolymer and MgO NPs through hydrogen bonding. The presence of hydroxyl groups on the surface of the cellulose biopolymer causes a negative charge on its surface. On the other hand, MgO NPs have a

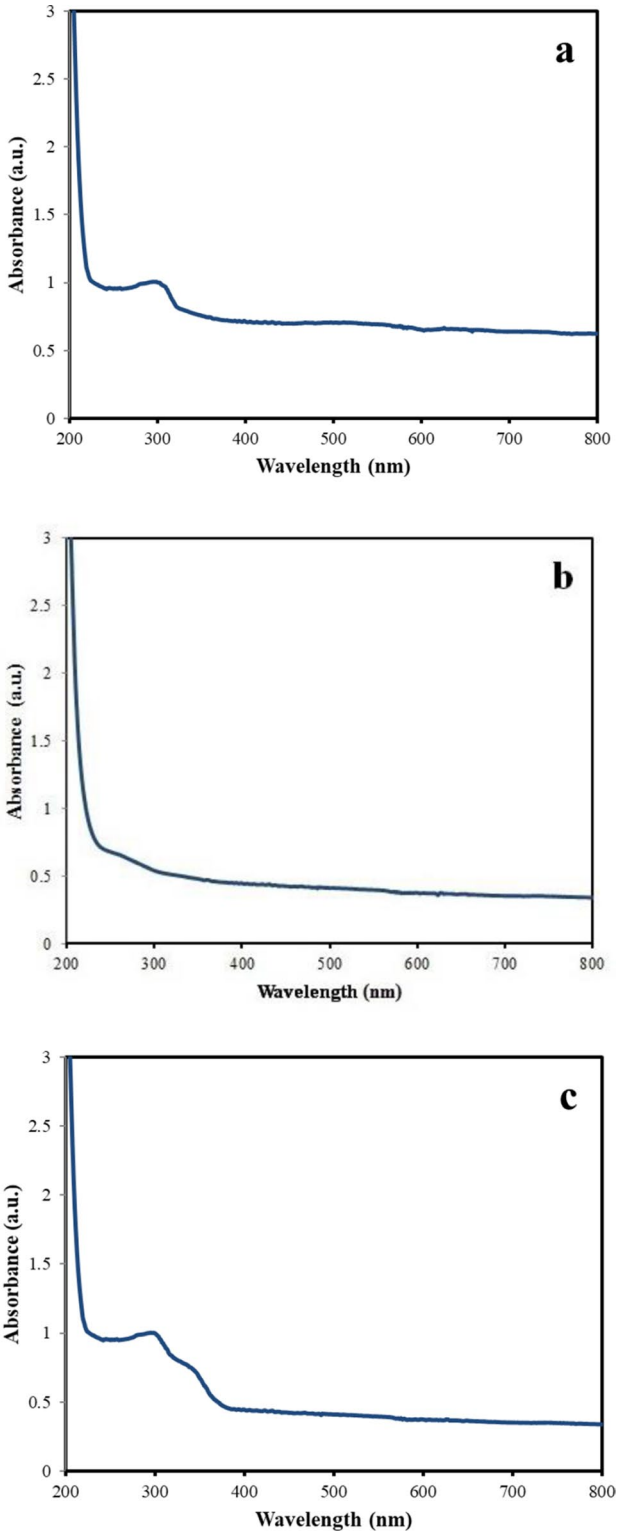

Fig. 1 UV–vis spectral analysis of the MgO NPs (**a**), cellulose biopolymer (**b**) and cellulose-MgO nanocomposite (**c**)

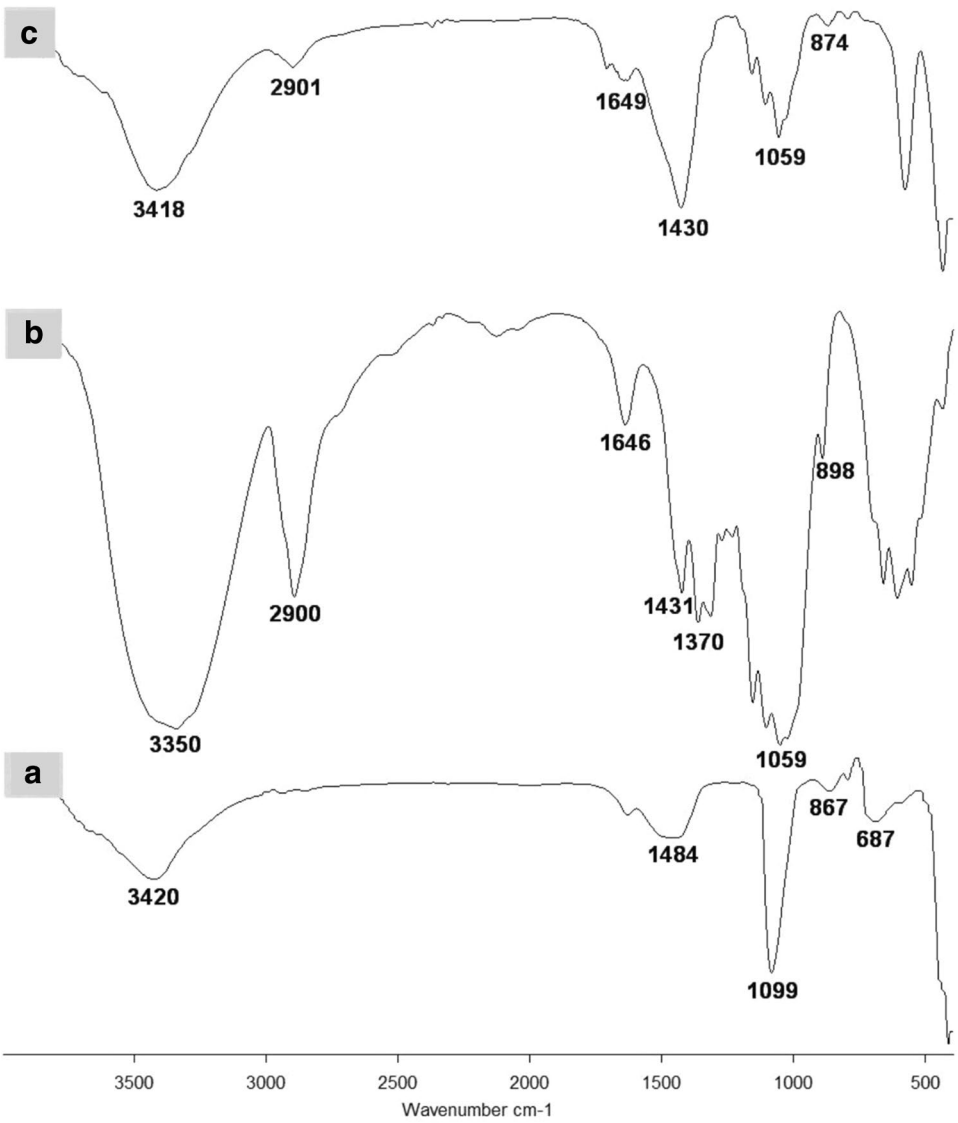

Fig. 2 FTIR spectra of **a** MgO NPs, **b** cellulose biopolymer and **c** cellulose-MgO nanocomposite

positive charge on their surface, which causes interactions between nanoparticles and biopolymer and the formation of cellulose-MgO nanocomposite [27].

X-ray Diffraction Analysis

Phase formation and crystallography of samples of MgO NPs, cellulose biopolymer and cellulose-MgO nanocomposite were investigated using XRD (Fig. 3). The nature of the peaks in the XRD pattern of the MgO NPs was in accordance with JCDS 75-1525, which expresses the cubic structure of the synthesized nanoparticles [28]. The absence of additional peaks in the synthesized nanoparticles pattern indicates their high purity. The XRD spectrum of cellulose biopolymer showed a cellulose pattern with peaks in the range of 15, 22, and 34 degrees, which showed the specification of the plates (110), (200) and (004), respectively

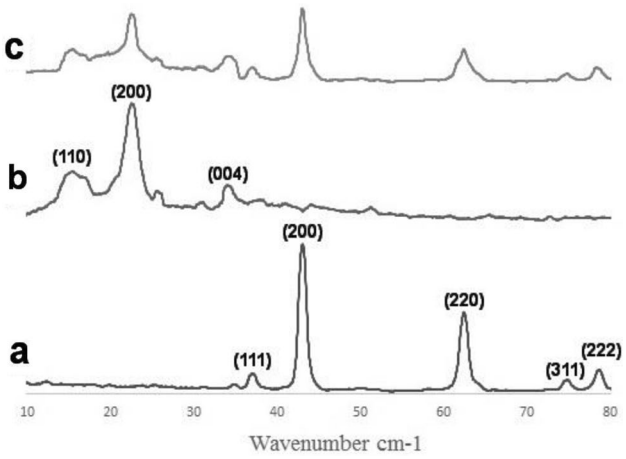

Fig. 3 X-ray diffraction (XRD) patterns of MgO NPs (a), cellulose biopolymer (b) and cellulose-MgO nanocomposite (c)

[29, 30]. The XRD pattern prepared from cellulose-MgO nanocomposite showed that it was affected by the structure of nanoparticles and biopolymer and confirmed the formation of the nanocomposite. Crystallite size of MgO NPs and cellulose were 19.7 nm and 31.7 nm, respectively.

SEM Analysis

The SEM images of MgO NPs, cellulose biopolymer and cellulose-MgO nanocomposites with different magnification (200 nm to 2 µm) are given in Fig. 4. Analysis of scanning electron micrograph represents the agglomeration of some of MgO NPs (Fig. 4a, b). These nanoparticles have a relatively uneven surface and spherical shape, which lead to providing further attraction sites and their better interaction. The size of 20 unagglomerated nanoparticles was calculated according to the size of the crystals and the histogram chart obtained from SEM micrographs, which their average was equal to 21 nm. Figure 4c and d revealed that networks with different pores have been created by cellulose fibers. The average diameter of synthesized bacterial cellulose fibers was about 14 nm. The interactions between the surface of MgO NPs and cellulose biopolymer led to the formation of cellulose-MgO nanocomposite (Fig. 4e, f). MgO NPs were dispersed randomly and uniformly in the nanocomposite and their agglomeration rate was decreased. The agglomeration was reduced due to creating links between the nanoparticles surface and the polymeric chains of cellulose.

Energy Dispersive X-Ray Analysis

For elemental analysis of MgO NPs, cellulose biopolymer and cellulose-MgO nanocomposite, the energy dispersive X-ray (EDX) detector on FESEM was used, and the results are presented in Fig. 5. The results revealed differences in composition of elements between cellulose biopolymer, MgO NPs and cellulose-MgO nanocomposite. The EDX pattern of MgO NPs only contained the elements of magnesium (56.88 wt%) and oxygen (43.12 wt%), and no other peak was observed for other elements, which suggests the purity of the synthesized MgO NPs. The EDX image of cellulose biopolymer indicated the presence of carbon and oxygen elements as 61.23 wt% and 43.12 wt%, respectively. The EDX pattern of cellulose-MgO nanocomposite contained magnesium (37.65 wt%), oxygen (33.12 wt%) and carbon (29.23 wt%). The existence of these elements together represented the formation of the nanocomposite. The cellulose biopolymer is rich in –OH and –C–O–O– groups and these groups can easily

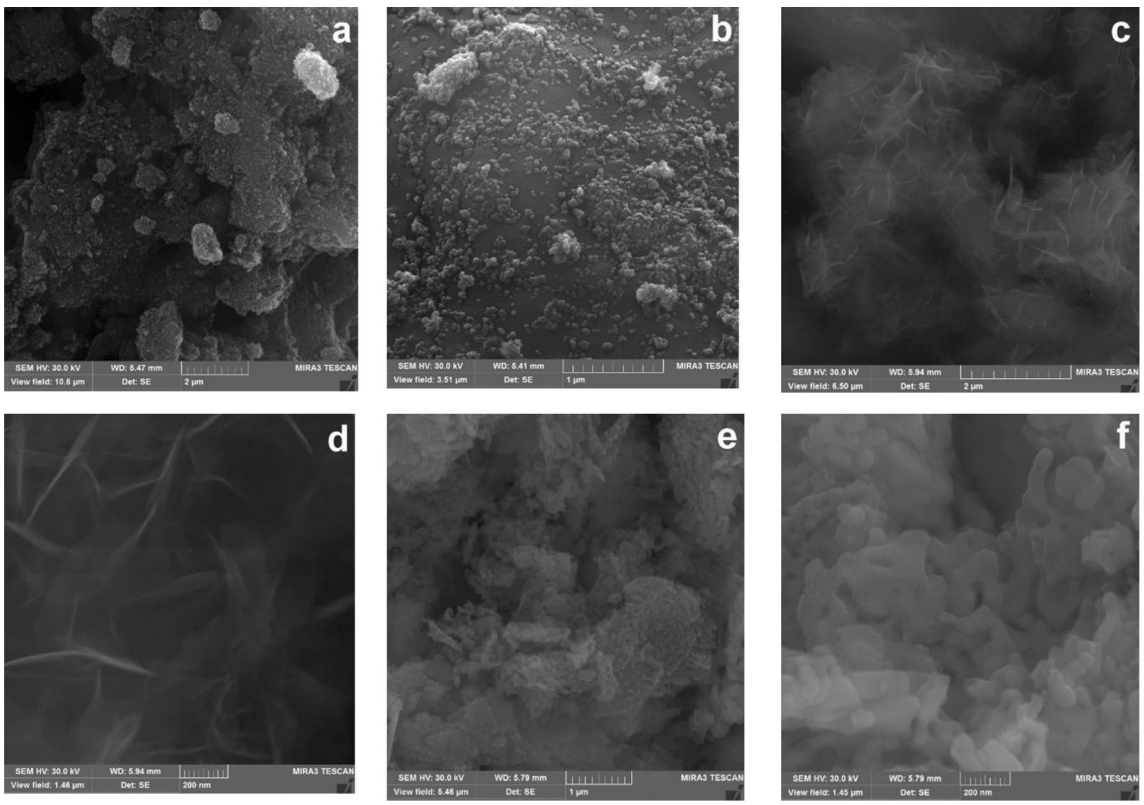

Fig. 4 Scanning electron microscopic micrographs of **a**, **b** MgO NPs, **c**, **d** cellulose biopolymer and **e**, **f** cellulose-MgO nanocomposite at low and high magnification

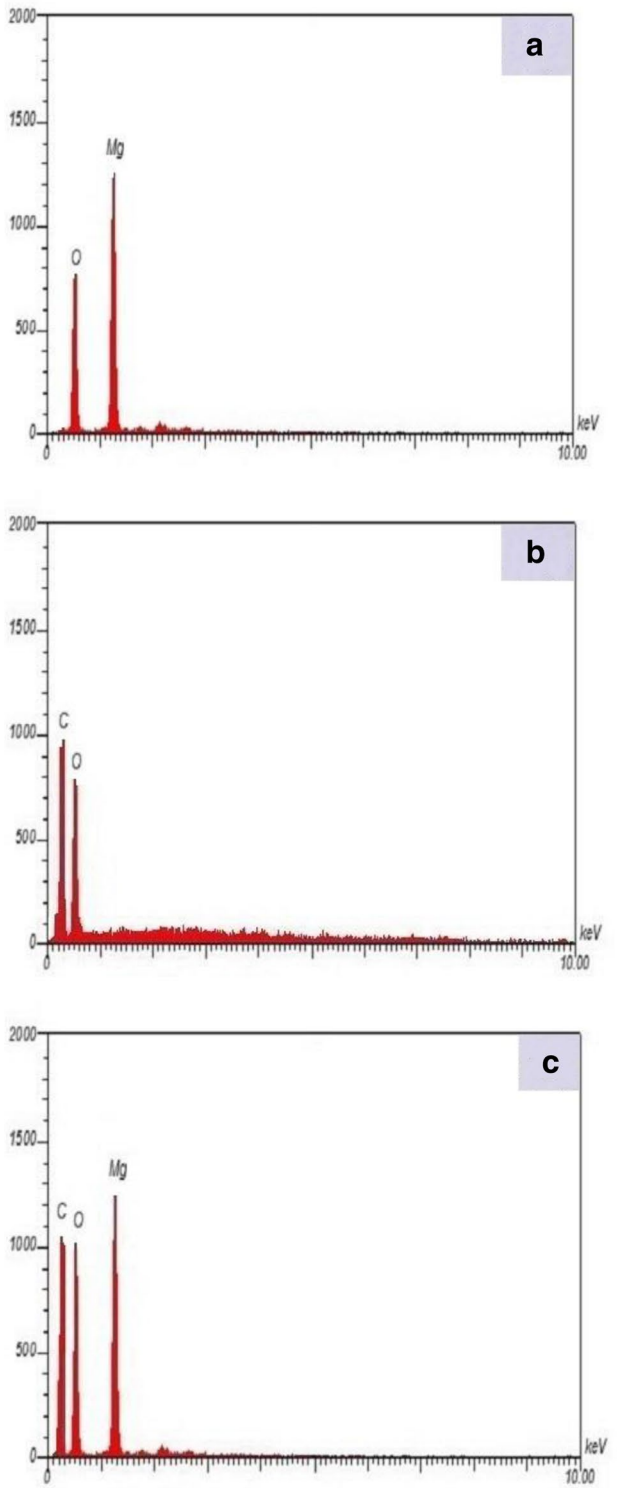

Fig. 5 Energy dispersive X-ray (EDX) spectra of **a** MgO NPs, **b** cellulose biopolymer and **c** cellulose-MgO nanocomposite

form firm links with the nanoparticles [31]. Therefore, the cellulose-MgO nanocomposite has sufficient strength for use in various fields.

TEM Analysis

Structure and morphology of cellulose-MgO nanocomposite was evaluated using transmission electron microscopy (Fig. 6). Nanocomposite images express the interactions between the surface of the MgO NPs and the cellulose biopolymer and confirm the formation of the cellulose-MgO nanocomposite. The synthesized MgO NPs had a relatively spherical structure and distributed within the cellulose biopolymer matrix. According to the TEM images obtained from cellulose-MgO nanocomposite, the amount of agglomerated nanoparticles was reduced.

Antifungal Activity Analysis

Based on Taguchi method, nanocomposites were synthesized using different amounts of MgO NPs, cellulose biopolymer and different stirring times. They were applied against fungus *Aspergillus niger* to detect the strongest antifungal compound. The antifungal activity of each of the synthesized nanocomposites is presented in Table 1. The results indicated that the nanocomposite produced using 4 mg/ml MgO NPs, 1 mg/ml cellulose and 90 min stirring time (experiment 5) had the highest inhibitory effect on fungal growth by 85.03% against the *Aspergillus niger*. The lowest inhibition of fungal growth was related to the synthesized nanocomposites under conditions of test 1 (2 mg/ml MgO NPs, 0.5 mg/ml cellulose and 30 min stirring time) as 41.38%.

The results of comparison of antifungal activity of cellulose-MgO nanocomposite with cellulose polymer and MgO NPs using two methods CFU and disk diffusion are presented in Table 2. In the CFU method, the antifungal activity of the MgO NPs against *Aspergillus niger* was 59.37% and cellulose biopolymer did not show antifungal activity. In this method, cellulose-MgO nanocomposite inhibited the growth of fungi by 85.03%, which was an improvement compared to its components. By using the disk diffusion method, the amount of growth inhibition zone was measured and its amount for MgO NPs against *Aspergillus niger* was 10 mm and the cellulose biopolymer did not show antifungal activity. The amount of growth inhibition zone for cellulose-MgO nanocomposite was 15 mm, which was more than its components (Fig. 7).

In accordance with the results of this study, previous studies also reported that the formation of nanocomposite improves its antimicrobial properties compared to its components [32, 33]. Cellulose biopolymer was used as a matrix to improve the antifungal properties of copper NPs, which showed satisfactory results [34]. Interaction between hydroxyl groups of cellulose biopolymer with negative charge and metal NPs with positive charge on their surface led to the formation of stable nanocomposites that prevented

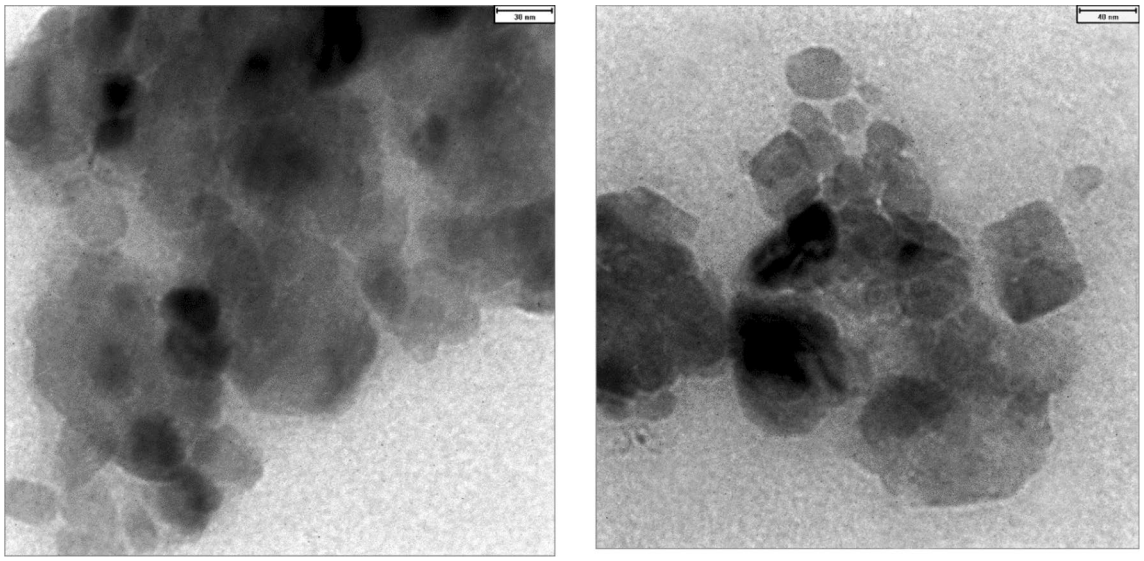

Fig. 6 Transmission electron microscope images of cellulose-MgO nanocomposite

Table 2 Antifungal activity of cellulose polymer, MgO NPs and cellulose-MgO nanocomposite

Factors	Fungal growth inhibition (%)	Zone of inhibition (mm)
MgO	59.37	10
Cellulose	0	0
Cellulose-MgO	85.03	15

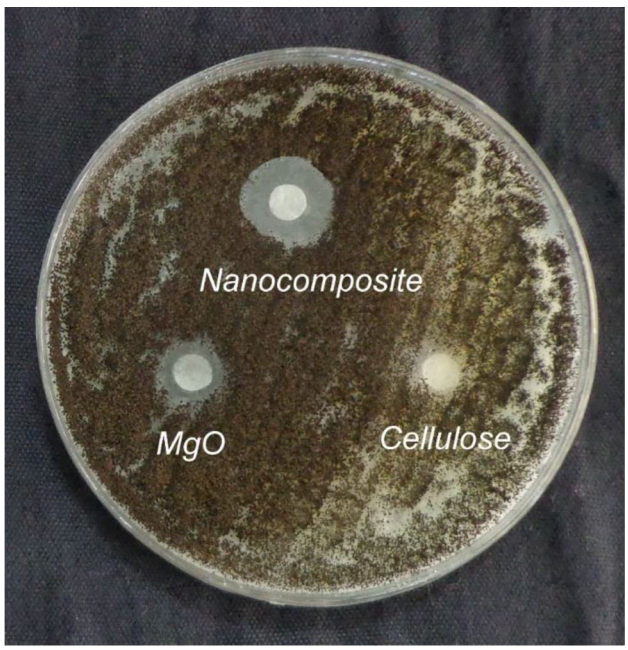

Fig. 7 Comparison of inhibition zone of the cellulose biopolymer, MgO NPs and cellulose-MgO nanocomposite against *Aspergillus niger*

the agglomeration of nanoparticles and thus their effective surface was increased [35]. This can lead to more contact between nanoparticles and fungi and can improve the effectiveness of nanoparticles against fungi. MgO NPs alone and in the form of nanocomposites exhibit favorable antifungal activity [36, 37]. The main mechanisms of action of MgO NPs against fungi are well known: (1) damage to membranes of fungi, (2) induction of oxidative stress, (3) release of toxic ions of Mg^{2+} and (4) disruption in the activity of organelles. The potential mechanisms illustrated in Fig. 8 are based on the results of previous research [38, 39].

The effect of MgO NPs, cellulose biopolymer and stirring time at different levels on growth inhibition of fungi are presented in Table 3. The second level in all three investigated factors showed the greatest effect on growth inhibition of *Aspergillus niger* fungi. The effect of MgO NPs, cellulose biopolymer and stirring time on the structure of cellulose-MgO nanocomposite on growth inhibition of fungus *Aspergillus niger* were 75.5%, 73.73%, and 72.59%, respectively.

Table 4 shows the interactions between MgO NPs, cellulose biopolymers and stirring time at different levels. The second level of cellulose biopolymer and the third level of stirring time had the highest interaction effect on growth inhibition of fungus *Aspergillus niger* as 46.43%. The MgO NPs at the second level and stirring time at the third level showed a significant interaction (20.03%) for inhibiting the growth of the fungus. The interaction between the second levels of MgO NPs and cellulose biopolymer showed the

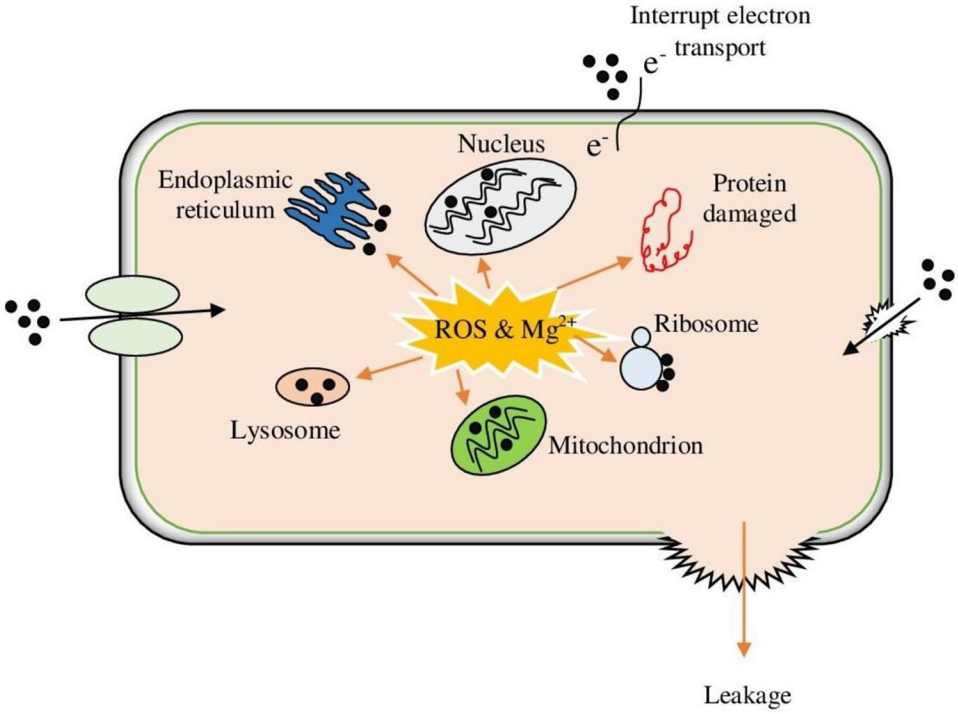

Fig. 8 Schematic mechanisms for antifungal activity of cellulose-MgO nanocomposite

Table 3 The main effects of different levels of MgO NPs, cellulose biopolymer and the stirring time on growth inhibition of *Aspergillus niger*

Factors	Level 1	Level 2	Level 3
MgO	50.30	75.50	67.04
Cellulose	54.08	73.73	65.03
Stirring time	60.72	72.59	59.52

Table 4 The interactions effects of studied factors on growth inhibiting of *Aspergillus niger*

Interacting factor pairs	Column	Severity Index (%)	Optimum conditions
Cellulose × Stirring time	2×3	46.43	[2, 3]
MgO × Stirring time	1×3	20.03	[2, 3]
MgO × Cellulose	1×2	11.93	[2]

lowest effect on the inhibition of growth of fungus *Aspergillus niger* by 11.93%.

The analysis of variance of MgO NPs, cellulose biopolymer and stirring time on inhibition of the growth of *Aspergillus niger* fungi are shown in Table 5. The MgO NPs by 42.72% and stirring time by 9.19% had the highest and lowest effects on growth inhibition of fungus *Aspergillus niger*, respectively. Cellulose biopolymer was also effective in reducing fungal growth by 22.58%.

In Table 6, optimum conditions for the production of cellulose-MgO nanocomposites with the highest antifungal activity have been predicted using the Taguchi method. Based on the results, the second levels of factors of MgO NPs, cellulose biopolymer and stirring time with the contribution of 11.22%, 9.45%, and 8.31%, respectively, had the highest role in improving the growth inhibition of *Aspergillus niger* fungi. According to the mean of growth inhibition rate of fungus *Aspergillus niger* by 64.28% in different experiment conditions and the decrease of

Table 5 The analysis of variance of factors affecting the growth inhibition of *Aspergillus niger*

Factors	DOF	Sum of squares	Variance	F-ratio (F)	Pure sum	Percent (%)
MgO	2	986.56	493.28	7.7	858.45	42.72
Cellulose	2	581.91	290.95	4.54	453.79	22.58
Stirring time	2	312.83	156.42	2.44	184.72	9.19

DOF degree of freedom

Table 6 The optimum conditions for the synthesis of cellulose-MgO nanocomposite with the highest antifungal activity

Factors	Level	Contribution
MgO	2	11.22
Cellulose	2	9.45
Stirring time	2	8.31
Total contribution from all factors		28.98
Current grand average of performance		64.28
Fungal growth inhibition at optimum condition		93.26

its growth rate in optimal conditions by 28.98%, fungus *Aspergillus niger* growth was expected to be reduced by 93.26% in optimum conditions to synthesize nanocomposite. Utilization of a suitable stirring time is important to obtain proper dissolution and stability of the solution for the formation of nanoparticles with the appropriate size. Previous studies have reported that the antimicrobial activity of nanoparticles increased with decreasing particle size and enhancement their concentration [40, 41].

Conclusions

In this study, cellulose-MgO nanocomposite was introduced as a biocompatible compound with desired antifungal activity. To determine the most favorable conditions for the synthesis of cellulose-MgO nanocomposite, 9 experiments were designed using Taguchi method and the bionanocomposite synthesized in experiment 5 (4 mg/ml MgO, 1 mg/ml cellulose and 90 min stirring time) showed the highest antifungal activity against the *Aspergillus niger*. In addition, the results indicated that the antifungal activity of cellulose-MgO nanocomposites was improved compared to its components. The characterizations of products were studied by UV–Vis, FTIR, XRD, SEM, EDX and TEM analyzes. The results of the structural analysis, including phase identification, crystal structure, chemical properties, appearance, and particle size, confirmed the formation of cellulose-MgO nanocomposite and improvement of its characterization. Therefore, the formation of nanocomposite with an increase in the contact surface of MgO NPs improves the antifungal activity of these nanoparticles. Considering the acceptable antifungal activity of cellulose-MgO nanocomposite, its usage is recommended in various fields.

Funding The authors declare no competing financial interest.

Code Availability 'Not applicable'.

Declarations

Conflict of interest The authors declare no conflicts of interest.

References

1. Maia FR, Reis RL, Oliveira JM (2020) Finding the perfect match between nanoparticles and microfluidics to respond to cancer challenges. Nanomedicine 24:102139. https://doi.org/10.1016/j.nano.2019.102139
2. Rezaei R, Safaei M, Mozaffari HR, Moradpoor H, Karami S, Golshah A, Salimi B, Karami H (2019) The role of nanomaterials in the treatment of diseases and their effects on the immune system. Open Access Maced J Med Sci 7:1884–1890. https://doi.org/10.3889/oamjms.2019.486
3. Mozaffari HR, Zavattaro E, Abdolahnejad A, Lopez-Jornet P, Omidpanah N, Sharifi R, Sadeghi M, Shooriabi M, Safaei M (2018) Serum and salivary IgA, IgG, and IgM levels in oral lichen planus: a systematic review and meta-analysis of case-control studies. Medicina 54:99. https://doi.org/10.3390/medicina54060099
4. Gao W, Zhang L (2021) Nanomaterials arising amid antibiotic resistance. Nat Rev Microbiol 19:5–6. https://doi.org/10.1038/s41579-41020-40420-41571
5. Laxminarayan R, Sridhar D, Blaser M, Wang M, Woolhouse M (2016) Achieving global targets for antimicrobial resistance. Science 353:874–875. https://doi.org/10.1126/science.aaf9286
6. Shishodia SK, Tiwari S, Shankar J (2019) Resistance mechanism and proteins in *Aspergillus* species against antifungal agents. Mycology 10:151–165. https://doi.org/10.1080/21501203.2019.1574927
7. Taran M, Safaei M, Karimi N, Almasi A (2021) Benefits and application of nanotechnology in environmental science: an overview. Biointerface Res Appl Chem 11:7860–7870. https://doi.org/10.33263/BRIAC111.78607870
8. Ali A, Shahid MA (2019) Polyvinyl alcohol (PVA)–*Azadirachta indica* (neem) nanofibrous mat for biomedical application: formation and characterization. J Polym Environ 27:2933–2942. https://doi.org/10.1007/s10924-019-01587-9
9. Song R, Murphy M, Li C, Ting K, Soo C, Zheng Z (2018) Current development of biodegradable polymeric materials for biomedical applications. Drug Des Devel Ther 12:3117–3145. https://doi.org/10.2147/DDDT.S165440
10. George J, Sabapathi, SN (2015) Cellulose nanocrystals: synthesis, functional properties, and applications. Nanotechnol Sci Appl 8:45–54. https://doi.org/10.2147/NSA.S64386
11. Moradpoor H, Safaei M, Rezaei F, Golshah A, Jamshidy L, Hatam R, Abdullah RS (2019) Optimisation of cobalt oxide nanoparticles synthesis as bactericidal agents. Open Access Maced J Med Sci 7:2757–2762. https://doi.org/10.3889/oamjms.2019.747
12. Moradpoor H, Safaei M, Mozaffari HR, Sharifi R, Imani MM, Golshah A, Bashardoust N (2021) An overview of recent progress in dental applications of zinc oxide nanoparticles. RSC Adv 11:21189–21206. https://doi.org/10.1039/D0RA10789A
13. Nguyen NY, Grelling N, Wetteland CL, Rosario R, Liu H (2018) Antimicrobial activities and mechanisms of magnesium oxide nanoparticles (nMgO) against pathogenic bacteria, yeasts, and biofilms. Sci Rep 8:16260. https://doi.org/10.1038/s41598-018-34567-5
14. Rana S, Kalaichelvan PT (2013) Ecotoxicity of nanoparticles. ISRN Toxicol 2013:574648–59872. https://doi.org/10.1155/2013/574648

15. Rajabi A, Ghazali MJ, Mahmoudi E, Baghdadi AH, Mohammad AW, Mustafah NM, Ohnmar H, Naicker AS (2019) Synthesis, characterization, and antibacterial activity of Ag_2O-loaded polyethylene terephthalate fabric via ultrasonic method. Nanomaterials 9:450. https://doi.org/10.3390/nano9030450
16. Safaei M, Taran M, Jamshidy L, Imani MM, Mozaffari HR, Sharifi R, Golshah A, Moradpoor H (2020) Optimum synthesis of polyhydroxybutyrate-Co_3O_4 bionanocomposite with the highest antibacterial activity against multidrug resistant bacteria. Int J Biol Macromolec 158:477–485. https://doi.org/10.1016/j.ijbiomac.2020.04.017
17. Safaei M, Taran M, Imani MM, Moradpoor H, Rezaei F, Jamshidy L, Rezaei R (2019) Application of Taguchi method in the optimization of synthesis of cellulose-MgO bionanocomposite as antibacterial agent. Polish J Chem Technol 21:116–122. https://doi.org/10.2478/pjct-2019-0047
18. Jiang W, Hua X, Han Q, Yang X, Lu L, Wang X (2009) Preparation of lamellar magnesium hydroxide nanoparticles via precipitation method. Powder Technol 191:227–230. https://doi.org/10.1016/j.powtec.2008.10.023
19. Krishnamoorthy K, Moon JY, Hyun HB, Cho SK, Kim SJ (2012) Mechanistic investigation on the toxicity of MgO nanoparticles toward cancer cells. J Mater Chem 22:24610–24617. https://doi.org/10.1039/C2JM35087D
20. Nguyen VT, Flanagan B, Gidley MJ, Dykes GA (2008) Characterization of cellulose production by a *Gluconacetobacter xylinus* strain from Kombucha. Curr Microbiol 57:449–453. https://doi.org/10.1007/s00284-008-9228-3
21. Somanathan T, Krishna VM, Saravanan V, Kumar R, Kumar R (2016) MgO nanoparticles for effective uptake and release of doxorubicin drug: pH sensitive controlled drug release. J Nanosci Nanotechnol 169: 9421–9431. https://doi.org/10.1166/jnn.2016.12164
22. Jiazhi YA, Xiaoli LI, HUANG L, Dongping SU (2013) Antibacterial properties of novel bacterial cellulose nanofiber containing silver nanoparticles. Chin J Chem Eng 21:1419–1424. https://doi.org/10.1016/S1004-9541(13)60636-9
23. Rezaei M, Khajenoori M, Nematollahi B (2011) Synthesis of high surface area nanocrystalline MgO by pluronic P123 triblock copolymer surfactant. Powder Technol 205:112–116. https://doi.org/10.1016/j.powtec.2010.09.001
24. Jung HS, Lee JK, Kim JY, Hong KS (2003) Crystallization behaviors of nanosized MgO particles from magnesium alkoxides. J Colloid Interface Sci 259:127–132. https://doi.org/10.1016/S0021-9797(03)00034-1
25. Hadia NM, Mohamed HA (2015) Characteristics and optical properties of MgO nanowires synthesized by solvothermal method. Mater Sci Semicond Process 29:238–244. https://doi.org/10.1016/j.mssp.2014.03.049
26. Abdulkhani A, Marvast EH, Ashori A, Hamzeh Y, Karimi AN (2013) Preparation of cellulose/polyvinyl alcohol biocomposite films using 1-n-butyl-3-methylimidazolium chloride. Int J Biol Macromolec 62:379–386. https://doi.org/10.1016/j.ijbiomac.2013.08.050
27. Oprea M, Panaitescu DM (2020). Nanocellulose hybrids with metal oxides nanoparticles for biomedical applications. Molecules 25:4045. https://doi.org/10.3390/molecules25184045
28. Rao KG, Ashok CH, Rao KV, Chakra CS (2014) Structural properties of MgO nanoparticles: synthesized by co-precipitation technique. Int J Sci Res 2:43–46.
29. Maeda H, Nakajima M, Hagiwara T, Sawaguchi T, Yano S (2006) Bacterial cellulose/silica hybrid fabricated by mimicking biocomposites. J Mater Sci 41:5646–5656. https://doi.org/10.1007/s10853-006-0297-z
30. Kumar A, Negi YS, Choudhary V, Bhardwaj NK (2014) Characterization of cellulose nanocrystals produced by acid-hydrolysis from sugarcane bagasse as agro-waste. J Mater Phys Chem 2:1–8. https://doi.org/10.12691/jmpc-2-1-1
31. Zhao B, Shao Z (2012) From paper to paper-like hierarchical anatase TiO_2 film electrode for high-performance lithium-ion batteries. J Phys Chem C 116:17440–17447. https://doi.org/10.1021/jp305744c
32. Hu Y, Guo Q, Liu P, Zhu R, Lu F, Ramaswamy S, Wu Y, Xu F, Zhang X (2021) Fabrication of novel cellulose-based antibacterial film loaded with poacic acid against staphylococcus aureus. J Polym Environ 29:745–754. https://doi.org/10.1007/s10924-020-01915-4
33. Vignesh N, Suriyaraj SP, Selvakumar R, Chandraraj K (2021) Facile fabrication and characterization of zn loaded cellulose membrane from cotton microdust waste and its antibacterial properties—a waste to value approach. J Polym Environ. 29:1651–1662. https://doi.org/10.1007/s10924-020-02021-1
34. Llorens A, Lloret E, Picouet P, Fernandez A (2012) Study of the antifungal potential of novel cellulose/copper composites as absorbent materials for fruit juices. Int J Food Microbiol 158:113–119. https://doi.org/10.1016/j.ijfoodmicro.2012.07.004
35. Ramesh S, Kim HS, Kim JH (2017) Cellulose-polyvinyl alcohol-nanoTiO_2 hybrid nanocomposite: thermal, optical and antimicrobial properties against pathogenic bacteria. Polymer Plast Technol Eng. https://doi.org/10.1080/03602559.2017.1344851
36. Wani AH, Shah MAA (2012) Unique and profound effect of MgO and ZnO nanoparticles on some plant pathogenic fungi. J Appl Pharm Sci 2:40–44
37. Sierra-Fernandez A, De la Rosa-Garcia SC, Gomez-Villalba LS, Gomez-Cornelio S, Rabanal ME, Fort R, Quintana P (2017) Synthesis, photocatalytic, and antifungal properties of MgO, ZnO and Zn/Mg oxide nanoparticles for the protection of calcareous stone heritage. ACS Appl Mater Interfaces 9:24873–24886. https://doi.org/10.1021/acsami.7b06130
38. He Y, Ingudam S, Reed S, Gehring A, Strobaugh TP, Irwin P (2016) Study on the mechanism of antibacterial action of magnesium oxide nanoparticles against foodborne pathogens. J Nanobiotechnol 14:54. https://doi.org/10.1186/s12951-016-0202-0
39. Cai L, Chen J, Liu Z, Wang H, Yang H, Ding W (2018) Magnesium oxide nanoparticles: effective agricultural antibacterial agent against *Ralstonia solanacearum*. Front Microbiol 9:790. https://doi.org/10.3389/fmicb.2018.00790
40. Tang ZX, Lv BF (2014) MgO nanoparticles as antibacterial agent: preparation and activity. Braz J Chem Eng 31:591–601. https://doi.org/10.1590/0104-6632.20140313s00002813
41. Chen J, Wu L, Lu M, Lu S, Li Z, Ding W (2020) Comparative study on the fungicidal activity of metallic MgO nanoparticles and macroscale MgO against soilborne fungal phytopathogens. Front Microbiol 11:365. https://doi.org/10.3389/fmicb.2020.00365